Control of sheared flow stabilized Z-pinch plasma properties with electrode geometry

E.L. Claveau[1], U. Shumlak[1], B.A. Nelson[1], A.D. Stepanov[1], Y. Zhang[1]

[1] *University of Washington, Seattle, USA*

Introduction

The Fusion Z-pinch Experiment (FuZE) produces a 0.3 cm radius by 50 cm long Z-pinch between the end of the inner electrode of a coaxial plasma gun and an end wall 50 cm away. The plasma column is stabilized for thousands of instability growth times by an embedded radially-sheared axial plasma flow, a method proposed in [1] and demonstrated experimentally in other sheared flow-stabilized Z-pinch devices, ZaP and ZaP-HD [2]. Temperatures of 1-2 keV and peak densities of 1×10^{23} m^{-3} are obtained in a 200 kA Z-pinch sustained for 5-8 μs. Recently, FuZE demonstrated sustained generation of neutrons over thousands of instability growth times [3], suggesting its viability as a thermonuclear power plant for a future device operating at higher current.

The formation process of the Z-pinch and the sustainment of the sheared flow involve the acceleration of plasma down a coaxial accelerator into an assembly region. Figure 1 b) shows 4 frames of a visible light emission high speed camera. Figure 1 c) shows current contours illustrating the pinch spatio-temporal evolution. The downstream portion of the assembly region, the end wall, is in the upper part of the figure while the upstream portion, composed of the end of the coaxial accelerator, is in the lower section. From these images, it is clear plasma is propagating toward the coaxial accelerator, against the main axial flow imparted by the upstream plasma gun. This behavior suggests that stagnation occurs at the downstream boundary conditions.

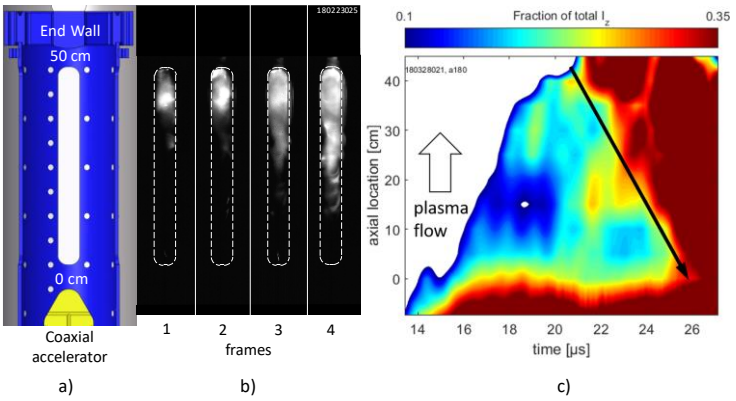

Figure 1. a), cross section of the FuZE Z-pinch region. b), four consecutive frames, separated by 1 μs interval, from the Kirana high speed camera showing visible light emission starting at the downstream section of the experiment and propagating toward the accelerator. c), contour between 10% and 35% of the total plasma current throughout the z-pinch assembly region. The backward propagating structure is indicated by the black arrow highlighting the high current edge starting at 50 cm and propagating upstream to reach the nose cone at 0 cm.

To investigate this effect, the transparency of the end wall was increased by changing its geometry and plasma pulses were performed at 4 and 5 kV charge voltage. The original "Hole-in" end wall is shown on Figure 2 alongside the Spoked end wall which has increased transparency. The ~ 60-fold increase in transparency was expected to permit more plasma to escape and prevent the stagnation effects shown in Figure 1.

Experimental Results

Pinch current is measured every 10 cm using arrays of 8 magnetic field probes. Each plot on Figure 3 shows the average current as well as a region encompassing one standard deviation above and below the average value, computed from the plasma pulses taken at the same experimental parameters. For both the 4 kV and 5 kV case, the current is virtually unchanged between the two end wall configurations for all axial locations up to 35 cm downstream of the nose cone. However, the current at 45 cm exhibits a net change for the 5 kV case, while no significant change is observed for the 4 kV case. This axial location is the closest magnetic field measurement to the end wall.

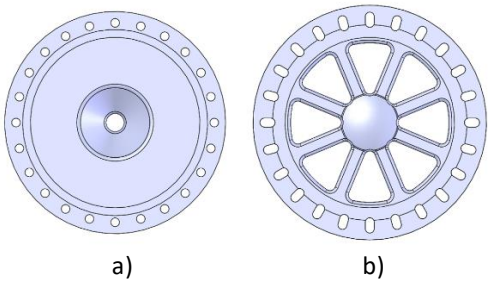

Figure 2. a) Original "Hole-in" end wall with a transparency of 1.12% and b) graphite Spoked end wall with a total transparency of 68.05%.

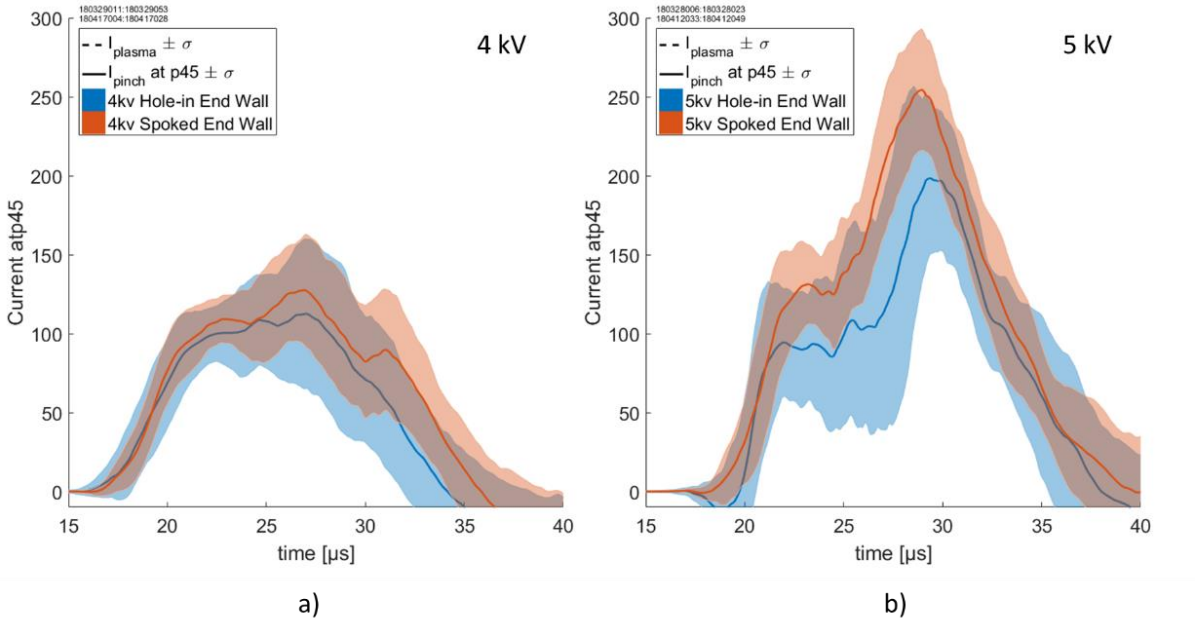

Figure 3. Mean (line) and standard deviation (shaded area) of total machine current and pinch current 45 cm downstream of the nose cone for the original (blue) and spoked (red) end wall for a) the 4 kV conditions and b) the 5 kV conditions.

Figure 4 shows the evolution of plasma velocity obtained from tracking the CIII and CV impurities for the 4 and 5 kV configurations. First, we observe that the CIII velocity progressively falls to zero as the pulse progresses. At that time, CV starts to appear, and its velocity tracks the previous CIII velocity. This can be explained if the CV emission is mainly from the hot flowing Z-pinch core while the CIII velocity comes from the cold, stagnated, outer edges. Average plasma densities are calculated with a He-Ne heterodyne quadrature interferometer. The 4 kV configuration has average densities between $1 - 3 \times 10^{21}$ m^{-3} while the 5 kV configuration has average densities between $3 - 8 \times 10^{21}$ m^{-3}.

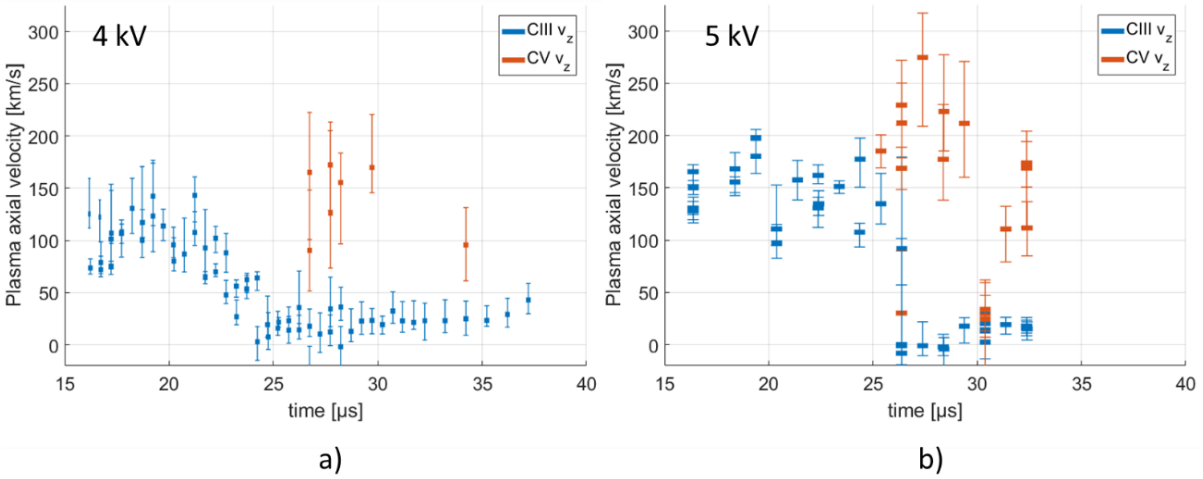

Figure 4. Plasma velocity temporal evolution obtained from tracking CIII (blue) and CV (red) impurities transitions using ion Doppler spectroscopy for the a) 4 kV and b) 5 kV conditions.

Analysis

Figure 5 shows the magnetic Reynolds number ($R_m = \frac{\mu_0 v_A L}{\eta}$) at the end wall calculated with Spitzer resistivity ($\eta = 5 \times 10^{-5} \ln \Lambda / T_e^{3/2}$) using T_e = 20 eV to T_e = 1000 eV. In all these cases, the value of R_m is above 1000, indicating that the plasma dynamic is dominated by advective effects. Therefore, the plasma can be considered to have frozen-in flux. As the end wall is the last section of the flux conserver, acting as the anode of the FuZE apparatus, the flux cannot escape past its physical boundary. Therefore, if the magnetic flux stays confined to the inside of the electrode, the plasma has to follow. This explains why no significant difference in total current was found along most of the Z-pinch length from increasing the end wall transparency.

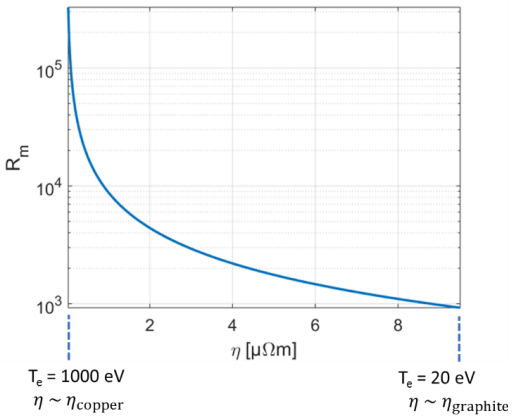

Figure 5. Magnetic Reynolds number at the end wall for plasma Spitzer resistivity calculated from T_e = 20 eV to T_e = 1000 eV.

For the original Hole-in end wall (Figure 2 a), most of the plasma flow was blocked by the presence of a solid boundary. For the Spoked end wall (Figure 2 b), the plasma has to be contained by the magnetic tension force acting between the spokes. The effectiveness of the axial confinement can be quantified from the ratio of the main outward force, the ram pressure, and a measure of the strength of the magnetic field, the magnetic field pressure.

Some current change was observed for the 5 kV conditions in Figure 3 while the currents were virtually the same for the 4 kV conditions. Using the interferometry data (ρ), average velocity obtained from Figure 4 (v_z) and magnetic field data obtained 15 cm from the end wall (B), we can calculate $\beta_{ram} = \frac{\rho v_z^2}{B^2/2\mu_0}$. Figure 6 shows the temporal evolution of that ratio with the same vertical scale. It is seen that for the 5 kV conditions, shown on Figure 6 b), the ratio greatly exceeds unity for the first 5 μs after plasma arrival. For the 4 kV case, the ram pressure and the magnetic pressure are of the same order as soon as the plasma reaches that axial location.

In conclusion, while the plasma has frozen-in flux, a part of it can still escape if the ram pressure greatly exceeds the magnetic field pressure close to the end wall. Therefore, an increase of transparency at the anode only affects the plasma properties if $\beta_{ram} \gg 1$.

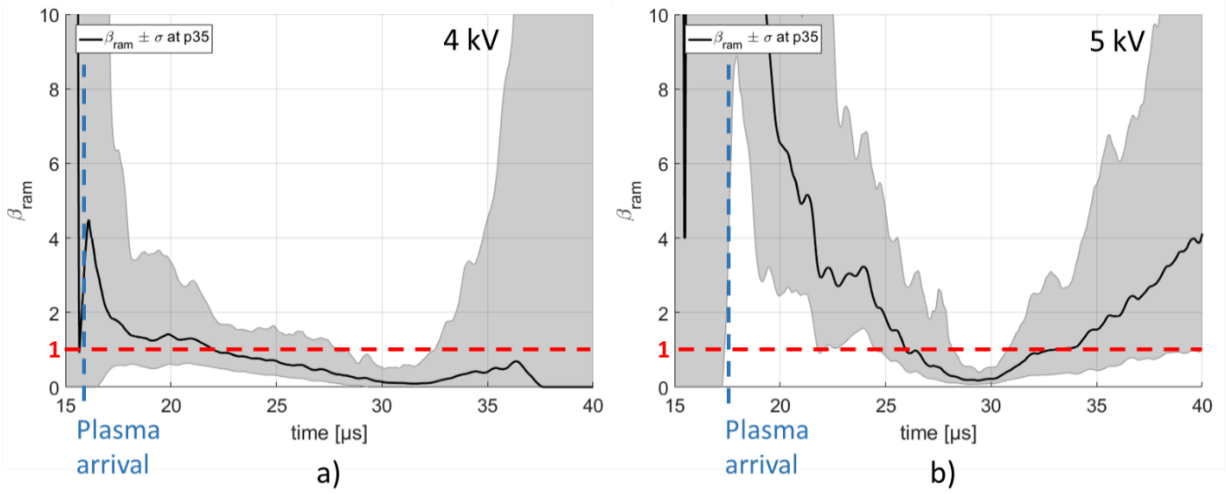

Figure 6. Temporal evolution of average beta obtained from the ratio of ram pressure to the magnetic field pressure for the a) 4kV conditions and b) 5 kV conditions.

References

[1] Shumlak, U., and C. W. Hartman. "Sheared flow stabilization of the m= 1 kink mode in Z pinches." Physical review letters 75.18 (1995): 3285.

[2] Shumlak, Uri, et al. "Increasing plasma parameters using sheared flow stabilization of a z-pinch." Physics of Plasmas 24.5 (2017): 055702.

[3] Zhang, Y., et al. "Sustained Neutron Production from a Sheared-Flow Stabilized Z Pinch." *Physical review letters* 122.13 (2019): 135001.